Hexahydro-1,3,5-trinitro-1,3,5-triazine Transformation by Biologically Reduced Ferrihydrite: Evolution of Fe Mineralogy, Surface Area, and Reaction Rates

ARTICLE *in* ENVIRONMENTAL SCIENCE AND TECHNOLOGY · AUGUST 2005

Impact Factor: 5.33 · DOI: 10.1021/es0490525 · Source: PubMed

4 AUTHORS:

Aaron Williams
South Tyneside NHS Foundation Trust
49 PUBLICATIONS **1,028** CITATIONS
SEE PROFILE

Kelvin B Gregory
Carnegie Mellon University
48 PUBLICATIONS **1,698** CITATIONS
SEE PROFILE

Gene F Parkin
University of Iowa
71 PUBLICATIONS **2,113** CITATIONS
SEE PROFILE

Michelle Scherer
University of Iowa
83 PUBLICATIONS **4,112** CITATIONS
SEE PROFILE

Environ. Sci. Technol. **2005**, *39,* 5183−5189

Hexahydro-1,3,5-trinitro-1,3,5-triazine Transformation by Biologically Reduced Ferrihydrite: Evolution of Fe Mineralogy, Surface Area, and Reaction Rates

AARON G. B. WILLIAMS, KELVIN B. GREGORY,† GENE F. PARKIN, AND MICHELLE M. SCHERER*

Department of Civil and Environmental Engineering, The University of Iowa, 4105 Seamans Center, Iowa City, Iowa 52242-1527

Microbial respiration of Fe(III) oxides has been shown to produce reduced Fe phases that are capable of transforming a variety of oxidized contaminants. Little data, however, are available on how these Fe phases evolve over time and how this evolution may affect their ability to reduce contaminants. Here, the evolution and reactivity of biologically reduced ferrihydrite were monitored over a period of 14 months. Solids were collected from a culture of *Geobacter metallireducens* (GS-15) that was incubated with ferrihydrite (as the electron acceptor) for 0, 7, 10, 20, 75, and 400 days. Mineralogical composition and surface area of the biologically reduced solids were characterized using Mössbauer spectroscopy, X-ray diffraction, and BET with N_2 adsorption. By day 10, ferrihydrite began to transform, and a nanoparticle magnetite/maghemite phase, as well as two ferrous phases, was observed. One of the ferrous phases was identified as siderite, whereas the other could not be positively identified. Likely candidates, however, include $Fe(OH)_2$(s) or an adsorbed Fe(II) species. Over the next few months, ferrihydrite was completely reduced and evolved into a mixture containing about 70% magnetite/maghemite, 19% siderite, and 11% of the second Fe(II) phase. The effect of incubation time on the reactivity of the biologically reduced solids was evaluated by measuring the kinetics of hexahydro-1,3,5-trinitro-1,3,5-triazine (RDX) transformation. The only products observed were the three reduced nitroso products. Rate coefficients (k) for RDX transformation were dramatically influenced by incubation time with half-lives of about 1 month observed in the presence of solids incubated for 10 and 20 days, 3 months with solids incubated for 75 days, and negligible removal with solids incubated for 400 days. The loss of reactivity was not directly correlated to any one mineralogical variable but may be due to particle size or surface chemistry changes in the reactive Fe phase or to cell die-off and the accumulation of cell lysis products after consumption of the electron acceptor. The dramatic effect of incubation time on the rate of RDX removal highlights a potential limitation of studying complex systems, as we have here, in batch reactors and suggests that incubation time is an important variable to consider when measuring and comparing rates of contaminant reduction.

Introduction

Microbial iron (Fe) respiration has a significant impact on the long-term development of anoxic subsurface environments (*1*, *2*). In soils and sediments that are not sulfidogenic, microbial reduction of iron is the principal mechanism of Fe(III) reduction, significantly influencing subsurface iron chemistry (*1*). The change in subsurface iron chemistry is largely a direct result of dissimilatory iron reducing bacteria (DIRB), who couple the oxidation of organic matter or H_2 to the reduction of Fe(III) to obtain energy for growth.

Although many crystalline Fe(III) oxides may be reduced by bacteria, ferrihydrite, a poorly crystalline Fe(III)-bearing mineral, has been suggested as the dominant form of bioavailable Fe(III) for microbial reduction in anoxic sediments (*3*−*5*). As such, ferrihydrite is often used as a model oxide to study the formation of secondary mineral phases produced by DIRB. The rate and extent of microbial iron reduction, as well as the composition of the resulting secondary mineral phases, are influenced by many factors including crystallinity, surface area, and particle size of the Fe(III) oxide, as well as solution pH, redox potential, and chemical composition (*4*, *6*−*10*). In addition to physical properties of the Fe(III) oxide, experimental variables, such as reactor design (i.e., batch or column) and mode of mixing also influence secondary mineral formation (*9*, *11*). Secondary minerals that are commonly observed include siderite ($FeCO_3$), magnetite (Fe_3O_4), vivianite ($Fe_3(PO_4)_2{\cdot}8H_2O$), green rust ($[Fe^{II}_{(6-x)}Fe^{III}_x(OH)_{12}]^{x+}[(A)_{x/n}{\cdot}H_2O]^{x-}$, where A is a n-valent anion), and maghemite (γ-Fe_2O_3) (*1*, *9*, *12*, *13*).

Secondary minerals formed from DIRB respiration have been shown to reduce many chemicals that are of significant environmental concern. More specifically, the formation of reduced, secondary mineral phases from microbial respiration has been linked to the transformation of nitroaromatics (*14*, *15*), chlorinated solvents (*13*, *16*, *17*), and pesticides (*18*, *19*). An important variable that does not appear to have been studied, however, is the effect of incubation time on the reactivity of biologically reduced solids. Although some of the chemistry of microbial ferrihydrite reduction has been studied, little is known about the evolution of mineral phases over time or how this evolution influences rates of contaminant reduction.

Here, we explore the evolution of secondary minerals during respiration of ferrihydrite by *Geobacter metallireducens* (GS-15) and evaluate how mineral evolution influences contaminant transformation rates using hexahydro-1,3,5-trinitro-1,3,5-triazine (RDX) as a probe compound. RDX is a high-energy explosive with numerous military applications (*20*−*22*). RDX is toxic, soluble, and mobile in groundwater and has a low affinity for the gas phase (*20*, *23*, *24*). Field data collected at the Iowa Army Ammunitions Plant in Middletown, IA have demonstrated that RDX is transformed via reductive processes (*25*). It is not clear, however, whether RDX transformation is the direct result of biological processes or whether abiotic reduction may be occurring. We have recently shown that Fe(II) associated with Fe-bearing minerals is capable of transforming RDX (*26*), and the presence of similar mineral phases from microbial Fe respiration led us to explore whether RDX transformation may also occur in the presence of DIRB.

* Corresponding author phone: (319) 335-5654; fax: (319) 335-5660; e-mail: michelle-scherer@uiowa.edu.

† Current address: Department of Microbiology, University of Massachusetts, 203 Morrill 4 North, Amherst, MA 01003.

10.1021/es0490525 CCC: $30.25
Published on Web 06/09/2005

To address the potential for biologically reduced Fe minerals to contribute to the natural attenuation of RDX, we (i) characterized the evolution of mineral phases formed from *G. metallireducens* respiration of ferrihydrite, (ii) quantified the reactivity of these oxides by measuring the extent and rate of RDX transformation at different incubation times, and (iii) compared mineral evolution and reactivity to better understand the complex biogeochemical interactions that may affect rates of contaminant transformation.

Experimental Section

Cell Culturing. Cultures of *G. metallireducens* were maintained with 20 mM acetate as the electron donor and 100 mM 2-line ferrihydrite as the electron acceptor. Fresh ferrihydrite was prepared by the rapid hydrolysis of a 0.4 M solution of $FeCl_3 \cdot 6H_2O$. A 10 M NaOH solution was used to raise the pH to 7.0 and induce the formation of a brown precipitate. The precipitate was allowed to mature under constant stirring for 2 h. After 2 h, the pH was checked again and readjusted to 7.0 with NaOH. The ferrihydrite was centrifuged (5000*g*) and washed in deionized water as necessary to remove chloride ions to below 1.0 mM as determined by ion chromatography. The mineral medium was prepared by adding 0.1 g of KCl, 0.2 g of NH_4Cl, and 0.6 g of NaH_2PO_4 to 800 mL of deionized water. Ten mL of mineral and vitamin solutions was then added as previously described (*1*). The solution pH was then adjusted to 6.8 using NaOH, and the final volume was brought to 900 mL with deionized water. Following pH and volume adjustment, 2 g of $NaHCO_3$ was added. The medium was immediately transferred to 138 mL serum bottles. Into each bottle, 90 mL of mineral medium and 10 mL of the 1.0 M 2-line ferrihydrite slurry was added. The serum bottles were sealed with a thick butyl stopper and bubbled with a continuous stream of anaerobic, sterile 80 N_2/20% CO_2 gas mixture for 30 min, after which the bottles were autoclaved.

Microbial Reduction of Ferrihydrite. Reduction of freshly precipitated ferrihydrite was initiated by inoculation with a 5% transfer of mid-log phase *G. metallireducens* actively growing on ferrihydrite. The reactor, a 138 mL serum bottle, contained 100 mL of growth medium and 100 mM ferrihydrite. The inoculated serum bottle was incubated at 30 °C. Biologically reduced solids were collected at 0, 7, 10, 20, 75, and 400 days under anoxic conditions and prepared for characterization and reaction with RDX as described next.

RDX Batch Experiments. All experiments were carried out in an anoxic chamber at room temperature (25 °C) on a rotary shaker at 40 rpm. The reactors were 120 mL, borosilicate glass serum bottles with aluminum crimps and Teflon-lined butyl rubber septa. Biologically reduced solids were separated from cell material by washing 4 times in deoxygenated 25 mM, pH 7.0 3-(*N*-Morpholino) propanesulfonic acid (MOPS) buffer. Each wash consisted of four steps: (i) suspending the solids plus cells in pH 7.0 MOPS buffer solution, (ii) physically agitating and sonicating the suspension for 10 min in an ice cooled bath (Fisher Scientific SF60), (iii) centrifuging the suspension for 5 min at 500 rpm, and (iv) decanting the supernatant. After the washing procedure was conducted 4 times, the biologically reduced solids were freeze-dried under anoxic conditions producing a fine powder.

Freeze-dried solids were weighed in the anoxic chamber and added to serum bottles to achieve a specific concentration (either 0.5 or 2.5 g/L) in 100 mL of medium. The medium consisted of aliquots of pH 7.0 MOPS buffer, which has a low tendency to complex Fe(II) (*27*, *28*). Experiments were initiated by the addition of RDX from an acetone stock solution. Samples were removed with a disposable syringe and needle and filtered through 0.2 μm filters into 2 mL amber autosampler vials. Experiments with ^{14}C-RDX were prepared in an identical fashion as described previously (*26*).

Mineral Characterization. Biologically reduced solids were characterized with Mössbauer spectroscopy, X-ray diffraction, and BET N_2 adsorption surface area analysis. Samples for Mössbauer spectroscopy measurements were prepared by withdrawing approximately 3 mL of aqueous suspension from each reactor inside the anoxic chamber and filtering with 0.2 μm filters to form a flat uniform wet paste. The filter paste and paper were removed from the filter housing and sealed between two pieces of Kapton tape to prevent oxidation during transfer from the anoxic chamber to the Mössbauer cryostat. Mössbauer spectra were collected in transmission mode with a constant acceleration drive system and a ^{57}Co source. Samples were mounted in either a top-loading Janis cryostat that used liquid cryogens or a top-loading Janis exchange-gas cryostat. Both systems maintained the source at room temperature during analysis. Data were calibrated with an α-Fe foil collected at room temperature. Examination of the data was completed with the Recoil software package using Voight based spectral fitting (University of Ottawa, Canada). Spectra collected on frozen samples ($T = 140$ K) were assumed to have a recoilless fraction of 1 ($f = 1$) when determining the percentage of Fe in each mineral.

Samples for XRD and BET analysis were freeze-dried under anoxic conditions with a constructed valve system to prevent oxygen exposure during transfer and attachment of the freeze-dry vial to the drying system. Samples of the dried powder were sieved (100 mesh) and mixed with small amounts of glycerol inside the anoxic chamber to help prevent oxidation during analysis. The glycerol−secondary mineral paste was smeared on a polycarbonate slide for XRD analysis. The specific surface area of the washed, freeze-dried solids was analyzed using a seven-point BET gas adsorption with N_2. A Quantachrome cell-seal assembly was used to prevent the oxidation of reduced solids during surface area analysis.

Chemical Analyses. ^{12}C-RDX, 1,3-dinitro-5-nitroso-1,3,5-triazacyclohexane (MNX), 1,3-dinitroso-5-nitro-1,3,5-triazacyclohexane (DNX), 1,3,5-trinitroso-1,3,5-triazacyclohexane (TNX), N_2O, NH_4^+, and ^{14}C-RDX were measured using methods previously described (*26*). Briefly, RDX and its nitroreduction intermediates were measured by HPLC (*29*). Gas chromatography of headspace samples was used to determine N_2O. NH_4^+ was determined by ion chromatography of filtered, liquid samples.

Results and Discussion

Characterization of Biologically Reduced Solids. Ferrihydrite and *G. metallireducens* were incubated at 30 °C for 0, 7, 10, 20, 75, and 400 days. Incubation times were selected to capture changes in the Fe mineralogy based on changes in the color of the mineral suspension. Visually, the ferrihydrite transformed rapidly starting on the seventh day of incubation. Between day 7 and day 10, the solids turned from a brown color, typical of ferrihydrite, to a black magnetic phase consistent with the rapid transformation of ferrihydrite previously reported in the presence of *Geobacter* and *Shewanella* species (*5*, *11*, *13*, *16*, *30*, *31*).

Mössbauer spectra of the filtered solids (not washed or freeze-dried) were collected at room temperature (RT, 295 K), 140 K, and liquid helium temperature (LHT, 4.2 K) at each incubation time. Spectra collected at RT and LHT indicate a complex mixture of Fe phases (Figures S1 and S2 of Supporting Information). Unfortunately, the RT and LHT spectra are difficult to resolve due to dynamic effects and subspectra overlap at RT and magnetic ordering of Fe(II) phases at LHT. Spectra collected at 140 K, however, reveal a distinct, rapid formation of new mineral phases by day 10 that continue to evolve until day 75 (Figure 1 and Table 1).

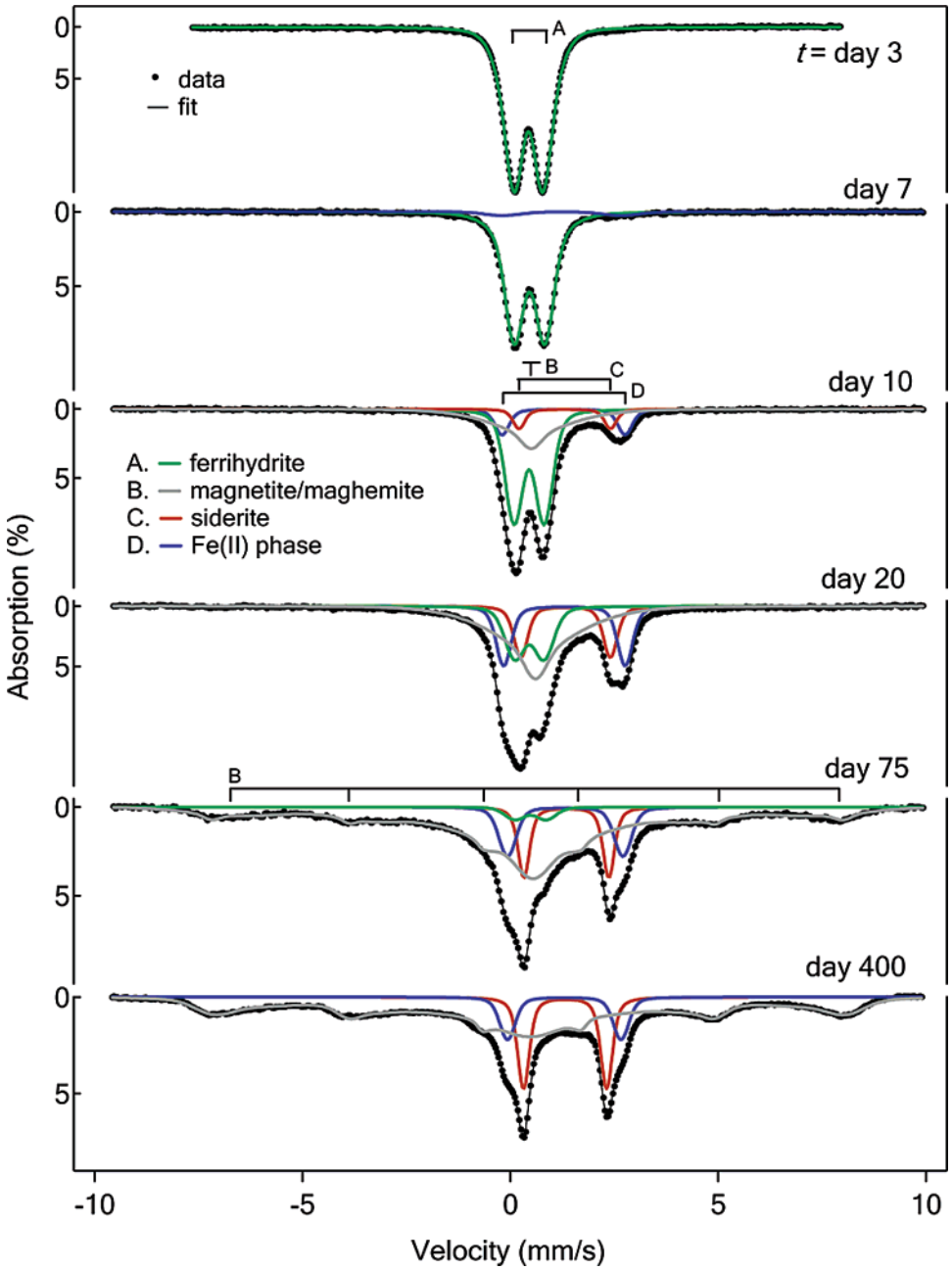

FIGURE 1. Mössbauer spectra of filtered, wet solids formed after incubation of *G. metallireducens* with ferrihydrite for different time periods. Spectra were collected at 140 K. Solids were not washed prior to spectra collection.

Initially, at day 0, only a single doublet (two absorption peaks labeled as subspectra A) is observed with spectral parameters that are consistent with ferrihydrite (*32*). At day 7, a trace amount of Fe(II) appears as a small doublet, and by day 10, two distinct Fe(II) phases are apparent as moderately sized doublets (subspectra C and D), in addition to a new, broad single peak at approximately 0.5 mm/s (subspectra B).

To help identify subspectra B, we collected additional spectra over a range of temperatures for the solids collected during day 75 (Figure 2). As the temperature is decreased from 295 to 140 K, the single peak begins to exhibit magnetic order based on the trace appearance of a sextet. At 50 and 4.2 K, the sextet becomes larger and more defined as the single peak decreases in area. This temperature-dependent behavior is consistent with size-dependent behavior of magnetic Fe oxides (i.e., superparamagnetism, or a loss of magnetic order once particles are smaller than the critical size needed to overcome thermal excitations). The superparamagnetic behavior observed for subspectra B suggests

TABLE 1. Mössbauer Spectral Parameters of Filtered, Wet Solids Formed after Incubation of *G. metallireducens* with Ferrihydrite for Different Time Periods (T = 140 K)[a]

	A. ferrihydrite		B. magnetite/maghemite			S. siderite		D. Fe(II) phase	
day	CS[b]	QSD[c]	CS	QSD	⟨H⟩[d]	CS	QSD	CS	QSD
0	0.44	0.77		ND[e]		ND		ND	
7	0.46	0.74		ND		ND		1.24	2.86
10	0.46	0.72	0.50	ND	ND	1.28	2.25	1.27	2.99
20	0.47	0.73	0.57	ND	ND	1.33	2.14	1.30	2.92
75	0.46	0.75	0.54	−0.05	42.7	1.35	2.04	1.32	2.78
400	ND		0.48	−0.03	44.5	1.32	2.00	1.30	2.73

[a] Spectra and subspectra are shown in Figure 1. [b] CS: center shift (mm/s). [c] QSD: quadrupole splitting distribution (mm/s). [d] ⟨*H*⟩: average magnetic splitting (T). [e] ND: not detected with Mössbauer spectroscopy.

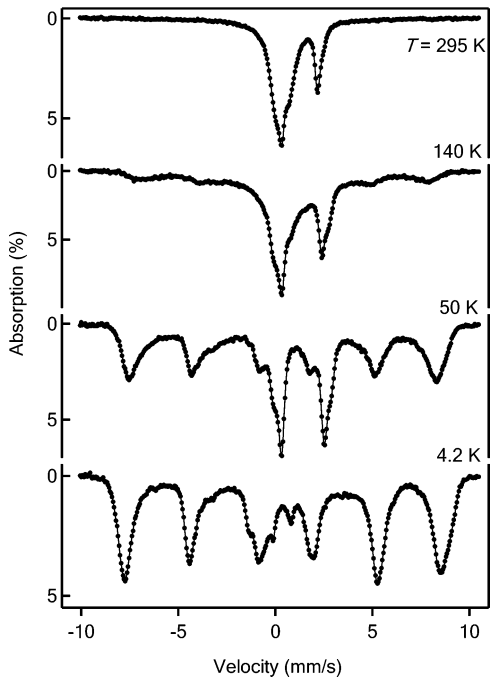

FIGURE 2. Effect of temperature on Mössbauer spectra of filtered, wet solids formed after incubation of *G. metallireducens* with ferrihydrite for 75 days. Solids were not washed or freeze-dried prior to spectra collection. As a visual aid, lines are used to connect the data points.

that the particles are less than 15 nm (*33*). XRD shows the presence of peaks that are consistent with both magnetite and maghemite in the biologically reduced solids (Figure S3 of Supporting Information), and a Raman spectra collected from another *G. metallireducens* culture identified maghemite as the dominant phase after 5 months incubation (data not shown). On the basis of XRD, Mössbauer spectroscopy, and Raman spectroscopy, subspectra B can reasonably be identified as nanoparticle magnetite or maghemite. The complexity of distinguishing between magnetite and maghemite in biologically reduced samples has been demonstrated with *G. metallireducens*, indicating that the reduced solids may in fact be a solid solution between the two end members (*12*). A similar conclusion, based on less than stoichiometric ratios of Fe(II)/Fe(III) expected for magnetite from anoxic acid digests of biogenic solids, was reached by McCormick et al. (*13*).

The first ferrous phase, indicated with subspectra C, is easily identified as siderite based on the center shift (CS) and quadruple splitting distribution (QSD) values obtained from spectral fitting of the Mössbauer data (CS = 1.22 mm/s and QSD = 1.86 mm/s at 295 K), as well as the XRD pattern (Figure S3 of Supporting Information) (*35*). Siderite is commonly reported to form under iron reducing conditions in the presence of carbonate (*9*, *34*−*36*). Carbonate concentrations were approximately 26 mM in the batch reactors, which is typical of the carbonate concentration used to culture *G. metallireducens* (*1*).

On the basis of XRD and Mössbauer spectra, it is difficult to positively identify the second Fe(II) phase (subspectra D) that appears at day 10 and persists through day 400. Despite the clear evidence of a second Fe(II) phase with Mössbauer spectroscopy, XRD does not indicate any additional Fe(II) phases other than siderite (Figure S3 of Supporting Information). This suggests that the Fe(II) phase, represented by subspectra D, is poorly crystalline or present at too low of a concentration to be observed with XRD. The percentage of the Fe(II) phase, however, is comparable to siderite, suggesting that the absence of an XRD signal is more likely

TABLE 2. Comparison of Mössbauer Spectral Parameters of the Fe(II) Phase Represented by Subspectra D in Figure 1 and Parameters Reported for $Fe(OH)_2$(s) and Adsorbed Fe(II) Species

	T (K)	CS (mm/s)	QSD (mm/s)	source
subspectra D[a]	295	1.17	2.50	this paper
	140	1.30	2.96	this paper
	50	1.35	2.98	this paper
	4.2	NA	NA	this paper
$Fe(OH)_2$(s)[b]	80	1.26	3.03	*45*
	150	1.28	2.97	*46*[c]
	90	1.25	3.00	*47, 48*
	77	NR	2.95	*49*
	77	1.27	3.05	*50*
adsorbed Fe(II)[d]	77	1.26	3.02	*37*
Al_2O_3 & TiO_2[e]	4.2	1.31−1.32	2.68−2.79	*41*
montmorillonite[f]	80	1.04	3.12	*42*

[a] Solids collected at day 20 in this work. [b] Line width (fwhm) = 0.32 mm/s. [c] Formed in the presence of green rust, line width (fwhm) = 0.32 mm/s. [d] Identified as Fe(II) adsorbed on illite based on a decrease in the spectral area of the Fe(II) doublet when exposed to oxygen. [e] ^{57}Fe(II) adsorbed on Al_2O_3 and TiO_2 at pH 7.4. [f] Fe(II) adsorbed on or in the interlayer of montmorillonite.

due to poor crystallinity. The Mössbauer parameters of the Fe(II) doublet measured at 140 K are within the range reported for $Fe(OH)_2$(s); however, room temperature measurements reveal QSD values that are significantly narrower than that expected for $Fe(OH)_2$(s) (Table 2). Another potential candidate is green rusts, which are structurally similar to $Fe(OH)_2$(s) and occasionally observed as a product of biological reduction. The lack of a clear Fe(III) green rust doublet to compliment the Fe(II) doublet, as well as the absence of green rust in the XRD pattern, however, does not support a green rust identification.

An alternative candidate for subspectra D is an Fe(II) species formed from adsorption to either an oxide or cell surface. Sorption of Fe(II) at oxide and cell surfaces is expected and has been estimated based on the recovery of Fe(II) after mild extraction or susceptibility of an Fe(II) phase to oxidation by oxygen (*7*, *9*, *11*, *34*−*40*). There are, however, only a limited number of studies that have characterized Fe(II) adsorbed at the oxide−water interface with Mössbauer spectroscopy (*41*−*43*), and we know of no studies that have characterized Fe(II) adsorbed at the cell−water interface with Mössbauer spectroscopy. For comparison, Table 2 shows the Mössbauer parameters reported for adsorbed Fe(II) in the literature and the parameters we measured for subspectra D at different temperatures. Interestingly, the Mössbauer parameters for the unidentified Fe(II) phase and those reported for Fe(II) adsorbed on Al_2O_3 and TiO_2, as well as an Fe(II) doublet observed from the reduction of illite by *Shewanella putrefaciens*, are reasonably similar, despite significant differences in experimental conditions (*37*, *41*). Mössbauer parameters of Fe(II) adsorbed on montmorillonite, however, differ from these numbers considerably, likely due to the proposed interlayer adsorption site in the clay structure (*42*). However, until a more thorough characterization of the Mössbauer spectra of adsorbed Fe(II) species is done, we can only speculate that the unidentified Fe(II) phase may be an adsorbed Fe(II) species.

RDX Transformation in the Presence of Biologically Reduced Solids. To evaluate the reactivity of the biologically reduced solids toward oxidized contaminants, we measured RDX transformation in the presence of 0.5 g/L washed, freeze-dried solids formed after three weeks incubation. In pH 7.0 MOPS buffer, 50 μM RDX was removed from solution after about 2 weeks with negligible RDX removal observed in the presence of ferrihydrite not incubated with *G. metallireducens* (Figure 3). MNX, DNX, and TNX appeared in order, suggesting

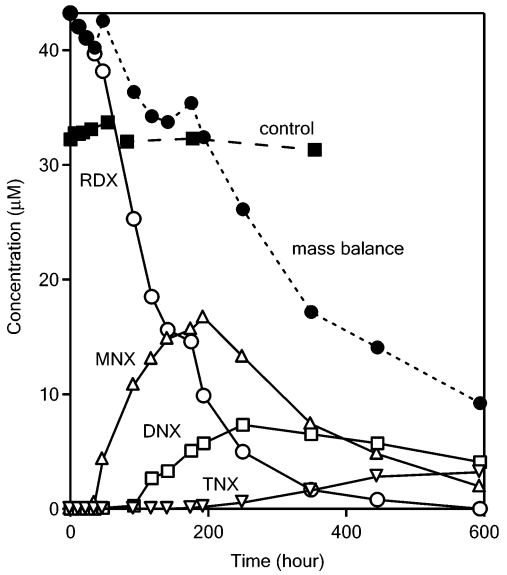

FIGURE 3. RDX transformation in the presence of solids formed after incubation of *G. metallireducens* for 21 days. Reactors contained 0.5 g/L freeze-dried solids, 50 mM pH 7.0 MOPS buffer, and an initial RDX concentration of 43 M. A control, ferrihydrite not incubated with *G. metallireducens*, did not exhibit any reduction of RDX.

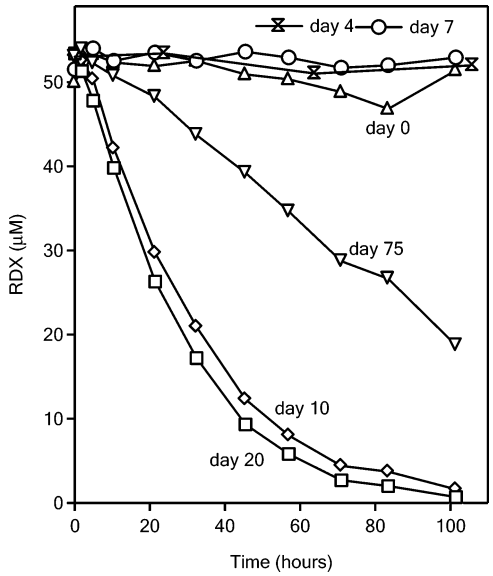

FIGURE 4. Effect of incubation time on RDX removal rates by washed solids formed in the presence of *G. metallireducens* and ferrihydrite. Reactors contained 2.5 g/L washed, freeze-dried solids, 50 mM pH 7.0 MOPS buffer, and an initial RDX concentration of 50−53 μM.

that sequential reduction of the nitro groups had occurred. The sum of the three nitroso derivatives of RDX, however, never comprised more than ~30% of the initial RDX, and the mass balance declined steadily throughout the experiment. Experiments with ^{14}C-RDX revealed negligible radioactivity associated with the solids (even after acetonitrile extraction and biooxidation) and less than 5% mineralization to CO_2. On the basis of our previous work with RDX degradation in the presence of Fe(II) on magnetite (*26*), we suspect that much of the remaining carbon mass balance may be formaldehyde, as an unidentified peak was observed in the aqueous phase on radio-chemical detector (RCD) chromatograms that accounted for as much as 60% of the initial ^{14}C-RDX. Trace amounts of NH_4^+ were found (about 6% of total N), and N_2O was analyzed for but not detected.

Effect of Incubation Time on RDX Transformation Rates. To assess the effect of incubation time on rates of RDX transformation, we measured rates of RDX removal in the presence of 2.5 g/L washed, freeze-dried solids collected after 0, 7, 10, 20, 75, and 400 days of incubation. We chose to separate the solids from the cells by a washing and sonication procedure because of previous work that used protein measurements to show that this procedure was sufficient to remove most of the cell material (*13*, *16*). We freeze-dried the solids to ensure an accurate mass of solid could be measured for each reactor. Clearly, minimal treatment of the solids is preferred, but a comparison of reactivity over time required removal of the cells as well as similar amounts of solid in each reactor. To check whether washing and freeze-drying altered the mineralogy of the solids, we compared Mössbauer measurements of a wet, unwashed sample and a washed, freeze-dried sample taken from the same reactor (Figure S4 of Supporting Information). The composition of the solids remained similar, but there was some increase in the magnetite/maghemite phase and a corresponding decrease in the siderite, ferrihydrite, and Fe(II) phases (presumably due to dissolution during washing) that may provide some bias toward the fine-grained magnetite/maghemite phase in the washed samples.

The washed, freeze-dried solids collected on days 0 and 7 resulted in negligible RDX removal (Figure 4). By days 10 and 20, however, complete removal of RDX was observed over a 5 day time period. The fast removal of RDX, however, was not sustained and decreased significantly for the solids collected at day 75. By day 400, the solids became unreactive, and negligible RDX removal was observed. Biologically reduced solids from a previous culture (used in Figure 2) showed a similar trend with RDX removal rates that were 10-fold faster on day 21 as compared to day 150 (data not shown). The only other work that we know of assessing the reactivity of aged biological solids showed that solids collected after 124 and 565 days of incubation exhibited no change in reactivity, which is consistent with our findings that dramatic changes in reaction rates are observed only at earlier times but inconsistent with our observation of negligible reactivity by day 400 (*16*).

Comparison of the Evolution of Fe Mineralogy, Surface Area, and Reactivity. The relationship between reactivity and mineralogy of the biologically reduced solids was explored by comparing the first-order rate coefficients for RDX removal (k_{obs}) to the mineralogical composition and surface area over time (Figure 5). The surface area of the biologically reduced solids decreased significantly over the first 20 days and then increased slowly until about day 75 when it reached a steady value (Figure 5B). In a multiphase system such as this, however, it is difficult to determine which phase is contributing most to the overall surface area measured. We anticipate that siderite would form fairly large crystals, whereas ferrihydrite and the magnetite/maghemite phase would have small crystals, and the increase in surface area at day 20 may reflect changes in the relative proportions of these minerals. The insight gained form surface area measurements is complicated due to their aggregate nature and the potential presence of surface coatings that may explain the unexpected observation that rates of RDX removal became slower at higher surface areas. The lack of relationship between surface area and rate of RDX removal suggests that the mineralogical composition may play a larger role than surface area in controlling the reactivity of biologically reduced solids toward oxidized contaminants.

A comparison of k_{obs} values and changes in mineralogical composition (Figure 5A,C) shows that the increase in reactivity of the biologically reduced solids over days 7−20 is associated with a decrease in ferrihydrite and initial formation of the Fe(II) species and nanoparticle magnetite/

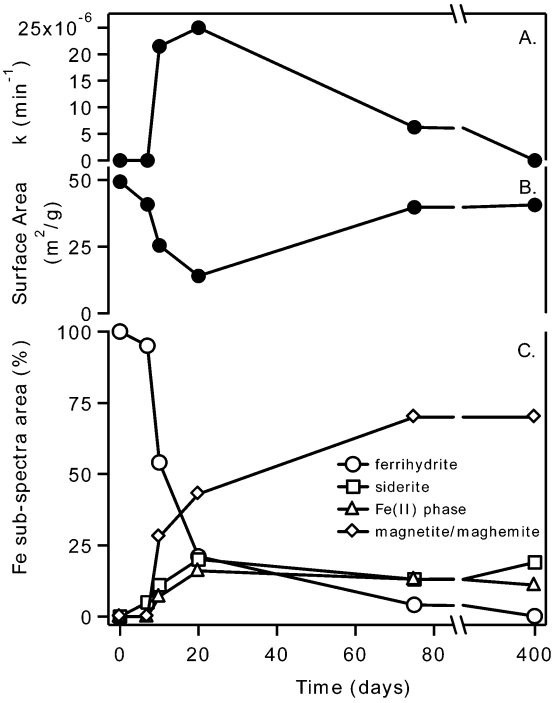

FIGURE 5. Comparison of first-order rate coefficients for RDX transformation, and surface area and iron mineralogy of solids formed during the incubation of ferrihydrite with *G. metallireducens*. Percentages of each Fe phase were determined by quantifying the area above each Mössbauer subspectrum in Figure 1 and dividing it by the total area of the spectrum.

maghemite. After day 20, the rate of RDX removal becomes significantly slower, while both Fe(II) species (siderite and the unidentified Fe(II) phase) remain fairly constant and the magnetite/maghemite phase continues to increase. There appears to be no strong correlation of k_{obs} values with changes in any of the mineral phases, making it difficult to identify the reactive Fe(II) phase. Up until day 20, however, it does appear that the increase in reactivity tracks the increases observed in the magnetite/maghemite phase, as well as the siderite and Fe(II) phase. If the magnetite/maghemite phase is the reactive phase, the decrease in reactivity between days 20 and 75 may be explained by an increase in particle size as indicated by the gradual transformation shown in Figure 1 (subspectra B) from a single peak, typical of a nanoparticle phase, to a sextet, indicating the formation of larger magnetic particles. Similar decreases in reactivity have been observed for synthetic magnetite over time (*44*). Another potential explanation is that by day 75, most of the ferrihydrite is reduced, and cell die-off may result in cell lysis products that affect the reactivity of the solids despite the extensive washing and sonication procedure.

Our findings suggest that active, continuous reduction of an Fe(III) oxide may be essential and limiting to a remediation strategy based on natural attenuation. With the increased reliance on natural attenuation as a viable remediation option, a better understanding of the complex biogeochemical interactions is critical. The dramatic effect of incubation time on rate of RDX removal also highlights a potential limitation of studying complex systems, as we have here, in batch reactors. At the minimum, our work suggests that incubation time is an important variable to consider when measuring rates of contaminant reduction, but, in a broader context, it seems clear that certain processes, such as the accumulation of Fe(II) species and particle size changes, need to be evaluated in flow-through reactors that are more representative of natural environments.

Acknowledgments

We would like to thank Derek Lovley (University of Massachusetts−Amherst) for providing us with a culture of *Geobacter metallireducens*, GS-15; Ben Bostick (Dartmouth College) for Raman spectroscopy analyses; and the Philip Larese-Casanova and the Central Microscopy Research Facility at The University of Iowa for help with Mössbauer spectroscopy measurements. This work was supported in part by the National Science Foundation under Grants BES-9983719 and DBI9602247, the U.S. Public Health Service Training Grant (732 GM8365) through The University of Iowa Center for Biocatalysis and Bioprocessing, as well as by the U.S. Department of Defense, through the Strategic Environmental Research and Development Program (SERDP). A.G.B.W. and K.B.G. contributed equally to this work.

Supporting Information Available

Additional data supporting our oxide characterization and the effect of washing the oxide. This material is available free of charge via the Internet at http://pubs.acs.org.

Literature Cited

(1) Lovley, D. R. Dissimilatory Fe(III) and Mn(IV) Reduction. *Microbiol. Rev.* **1991**, *55*, 259−287.

(2) Nealson, K.; Saffarini, D.; Moser, D.; Smith, M. J. A Spectrophotometric Method For Monitoring Tactic Responses of Bacteria Under Anaerobic Conditions. *J. Microbiol. Methods* **1994**, *20*, 211−218.

(3) Arnold, R. G.; DiChristina, T. J.; Hoffmann, M. R. Reductive Dissolution of Fe(III) Oxides by *Pseuomonas* sp 200. *Biotechnol. Bioeng.* **1986**, *32*, 1081−1096.

(4) Roden, E. E.; Zachara, J. M. Microbial Reduction of Crystalline Iron(III) Oxides: Influence of Oxide Surface Area and Potential for Cell Growth. *Environ. Sci. Technol.* **1996**, *30*, 1618−1628.

(5) Lovley, D. R.; Phillips, E. J. P. Rapid assay for microbially reducible ferric iron in aquatic sediments. *Appl. Environ. Microbiol.* **1987**, *53*, 1536−1540.

(6) Bell, P. E.; Mills, A. L.; Herman, J. S. Biogeochemical conditions favoring magnetite formation during anaerobic iron reduction. *Appl. Environ. Microbiol.* **1987**, *53*, 2610−2616.

(7) Roden, E. E.; Urrutia, M. M. Ferrous Iron Removal Promotes Microbial Reduction of Crystalline Iron(III) Oxides. *Environ. Sci. Technol.* **1999**, *33*, 1847−1853.

(8) Zachara, J. M.; Frederickson, J. K.; Shu-Mei, L.; Kennedy, D. W.; Smith, S. C.; Gassman, P. L. Bacterial reduction of crystalline Fe^{3+} oxides in single phase suspensions and subsurface materials. *Am. Mineral.* **1998**, *83*, 1426−1443.

(9) Fredrickson, J. K.; Zachara, J. M.; Kennedy, D. W.; Dong, H.; Onstott, T. C.; Hinman, N. W.; Li, S.-m. Biogenic iron mineralization accompanying the dissimilatory reduction of hydrous ferric oxide by a groundwater bacterium. *Geochim. Cosmochim. Acta* **1998**, *62*, 3239−3257.

(10) Royer, R. A.; Burgos, W. D.; Fisher, A. S.; Unz, R. F.; Dempsey, B. A. Enhancement of Biological Reduction of Hematite by Electron Shuttling and Fe(II) Complexation. *Environ. Sci. Technol.* **2002**, *36*, 1936−1946.

(11) Hansel, C. M.; Benner, S. G.; Neiss, J.; Dohnalkova, A.; Kukkadapu, R.; Fendorf, S. Secondary mineralization pathways induced by dissimilatory iron reduction of ferrihydrite under advective flow. *Geochim. Cosmochim. Acta* **2003**, *67*, 2977−2992.

(12) Hanzlik, M.; Petersen, N.; Keller, R.; Schmidbauer, E. Electron microscopy and ^{57}Fe Mössbauer spectra of 10 nm particles, intermediate in composition between Fe_3O_4 and Fe_2O_3, produced by bacteria. *Geophys. Res. Lett.* **1996**, *23*, 479−482.

(13) McCormick, M. L.; Adriaens, P. Carbon tetrachloride transformation on the surface of nanoscale biogenic magnetite particles. *Environ. Sci. Technol.* **2004**, *38*, 104−1053.

(14) Heijman, C. G.; Holliger, C.; Glaus, M. A.; Schwarzenbach, R. P.; Zeyer, J. Abiotic Reduction of 4-Chloronitrobenzene to 4-Chloroaniline in a Dissimilatory Iron-Reducing Enrichment Culture. *Appl. Environ. Microbiol.* **1993**, *59*, 4350−4353.

(15) Hofstetter, T. B.; Heijman, C. G.; Haderlein, S. B.; Holliger, C.; Schwarzenbach, R. P. Complete reduction of TNT and other (poly)nitroaromatic compounds under iron-reducing subsurface conditions. *Environ. Sci. Technol.* **1999**, *33*, 1479−1487.

(16) McCormick, M. L.; Bouwer, E. J.; Adriaens, P. Carbon tetrachloride transformation in a model iron-reducing culture: Relative kinetics of biotic and abiotic reactions. *Environ. Sci. Technol.* **2002**, *36*, 403−410.
(17) Fredrickson, J. K.; Gorby, Y. A. Environmental processes mediated by iron-reducing bacteria. *Curr. Opin. Biotechnol.* **1996**, *7*, 287−294.
(18) Xu, J. C.; Stucki, J. W.; Wu, J.; Kostka, J. E.; Sims, G. K. Fate of atrazine and alachlor in redox-treated ferruginous smectite. *Environ. Toxicol. Chem.* **2001**, *20*, 2717−2724.
(19) Cervini-Silva, J.; Kostka, J. E.; Larson, R. A.; Stucki, J. W.; Wu, J. Fate of atrazine and alachlor in redox-treated ferruginous smectite. *Environ. Toxicol. Chem.* **2003**, *20*, 1046−1050.
(20) Gong, P.; Hawari, J.; Thiboutot, A.; Ampleman, G.; Sunahara, G. I. Ecotoxicological effects of hexahydro-1,3,5-trinitro-1,3,5-triazine on soil microbial activities. *Environ. Toxicol. Chem.* **2001**, *20*, 947−951.
(21) Haas, R.; Schreiber, I.; Low, E.; Stork, G. Conception for the investigation of contaminated munitions plants 2. Investigation of former RDX plants and filling stations. *Fresenius J. Anal. Chem.* **1990**, *338*, 41−45.
(22) Bryd, J. J.; Hayes, K. F. 12th International Incineration Conference: Knoxville, TN, 1993.
(23) Robidoux, P. Y.; Svendsen, C.; Caumartin, J.; Hawari, J.; Ampleman, G.; Thiboutot, S. Chronic toxicity of energetic compounds in soil determined using the earthworm (*Eisenia andrei*) reproduction test. *Environ. Toxicol. Chem.* **2000**, *19*, 1764−1773.
(24) Yinon, J. Trace analysis of explosives in water by gas chromatography−mass spectrometry with a temperature-programmed injector. *J. Chromatogr.* **1996**, *742*, 205−209.
(25) Beller, H. R.; Tiemeier, K. Use of Liquid Chromatography/Tandem Mass Spectrometry to Detect Distinctive Indicators of In Situ RDX Transformation in Contaminated Groundwater. *Environ. Sci. Technol.* **2002**, *36*, 2060−2066.
(26) Gregory, K. B.; Larese-Casanova, P.; Parkin, G. F.; Scherer, M. M. Abiotic transformation of hexahydro-1,3,5-trinitro-1,3,5-triazine by Fe(II) bound to magnetite. *Environ. Sci. Technol.* **2004**, *38*, 1408−1414.
(27) Perlinger, J. A.; Buschmann, J.; Angst, W.; Schwarzenbach, R. P. Iron Porphyrin and Mercaptojuglone Mediated Reduction of Polyhalogenated Methanes and Ethanes in Homogeneous Aqueous Solution. *Environ. Sci. Technol.* **1998**, *32*, 2431−2437.
(28) Perrin, D. D.; Dempsey, B. *Buffers for pH and metal ion control*; Chapman and Hall: London, 1974.
(29) Oh, B. T.; Alvarez, P. J. J. Hexahydro-1,3,5-trinitro-1,3,5-triazine (RDX) degradation in biologically active iron columns. *Water Air Soil Pollut.* **2002**, *141*, 325−335.
(30) Lovley, D. R.; Coates, J. D.; Blunt-Harris, E. L.; Phillips, E. J. P.; Woodward, J. C. Humic substances as electron acceptors for microbial respiration. *Nature* **1996**, *382*, 445−448.
(31) Gregory, K. B. Ph.D. Thesis, Department of Civil and Environmental Engineering, The University of Iowa, Iowa City, 2002.
(32) Murad, E.; Johnston, J. H. Iron oxides and oxyhydroxides. In *Mössbauer spectroscopy applied to inorganic chemistry*; Long, G. J., Ed.; Plenum Publishers: New York, 1987; Vol. 2, pp 507−582.
(33) Morup, S.; Dumesic, J. A.; Topsoe, H. Magnetic microcrystals. In *Applications of Mössbauer Spectroscopy*; Cohen, R. L., Ed.; Academic Press: New York, 1980; Vol. II, pp 1−48.
(34) Kukkadapu, R.; Zachara, J. M.; Smith, S. C.; Frederickson, J. K.; Liu, C. Dissimilatory bacterial reduction of Al-substituted goethite in subsurface sediments. *Geochim. Cosmochim. Acta* **2001**, *65*, 2913−2924.
(35) Cooper, C. D.; Picardal, F.; Rivera, J.; Talbot, C. Zinc immobilization and magnetite formation via ferric oxide reduction by Shewanella 200 putrefaciens 200. *Environ. Sci. Technol.* **2000**, *34*, 100−106.
(36) Liu, C.; Kota, S.; Zachara, J. M.; Fredrickson, J. K.; Brinkman, C. K. Kinetic Analysis of the Bacterial Reduction of Goethite. *Environ. Sci. Technol.* **2001**, *35*, 2482−2490.
(37) Dong, H. L.; Kukkadapu, R. K.; Zachara, J. M.; Kennedy, D. W.; Kostandarithes, H. M. Microbial reduction of structural Fe(III) in illite and goethite. *Environ. Sci. Technol.* **2003**, *37*, 1268−1276.
(38) Benner, S. G.; Hansel, C. M.; Wielinga, B. W.; Fendorf, S. Reductive Dissolution and Biomineralization of Iron Hydroxide under Dynamic Flow Conditions. *Environ. Sci. Technol.* **2002**, *36*, 1705−1711.
(39) Roden, E. E.; Urrutia, M. M. Influence of Biogenic Fe(II) on Bacterial Crystalline Fe(III) Oxide Reduction. *Geomicrobiol. J.* **2002**, *19*, 209−251.
(40) Liu, C.; Zachara, J. M.; Gorby, Y. A.; Szecsody, J. E.; Brown, C. F. Microbial Reduction of Fe(III) and Sorption/Precipitation of Fe(II) on *Shewanella putrefaciens* Strain CN32. *Environ. Sci. Technol.* **2001**, *35*, 1385−1393.
(41) Williams, A. G. B.; Scherer, M. M. Spectroscopic Evidence for Fe(II)−Fe(III) Electron Transfer at the Fe Oxide−Water Interface. *Environ. Sci. Technol.* **2004**, *38*, 4782−4790.
(42) Diamant, A.; Pasternak, M.; Banin, A. Characterization of Adsorbed Iron in Montmorillonite by Mössbauer Spectroscopy. *Clays Clay Miner.* **1982**, *30*, 63−66.
(43) Ambe, S.; Okada, T.; Ambe, F. In situ Emission Mössbauer Studies on Carrier-Free $^{75}Co^{2+}$ and $^{119}Sb^{5+}$ Ions at Interfaces between Spinel-Type Oxides and Aqueous Solutions. *Radiochim. Acta* **1998**, *80*, 101−108.
(44) Klausen, J.; Trober, S. P.; Haderlein, S. B.; Schwarzenbach, R. P. Reduction of substituted nitrobenzenes by Fe(II) in aqueous mineral suspensions. *Environ. Sci. Technol.* **1995**, *29*, 2396−2404.
(45) Koch, C. B. Structures and properties of anionic clay minerals. *Hyperfine Interact.* **1998**, *117*, 131−157.
(46) Bocher, F.; Géhin, A.; Ruby, C.; Ghanbaja, J.; Abdelmoula, M.; Génin, J.-M. R. Coprecipitation of Fe(II−III) hydroxycarbonate green rust stabilized by phosphate adsorption. *Solid State Sci.* **2004**, *6*, 117−124.
(47) Miyamoto, H.; Shinjo, T.; Takada, T. Mössbauer effect of the ^{57}Fe in $Fe(OH)_2$. *J. Phys. Soc. Jpn.* **1967**, *23*, 1421.
(48) Miyamoto, H. The magnetic properties of $Fe(OH)_2$. *Mater. Res. Bull.* **1976**, *11*, 329−335.
(49) Rezel, D.; Bauer, P.; Genin, J. M. R. Superparamagnetic behavior and hyperfine interactions in ferrous hydroxide II and green rust I. *Hyperfine Interact.* **1988**, *42*, 1075−1078.
(50) Cardile, C. M.; Lewis, D. G. Mössbauer spectroscopic evidence of a $^{IV}Fe^{3+}$ intermediate in the oxidation of $Fe(OH)_2$ to α-FeOOH. *Aust. J. Soil Res.* **1991**, *29*.

Received for review June 22, 2004. Revised manuscript received April 6, 2005. Accepted April 14, 2005.

ES0490525